J Mol Model
DOI 10.1007/s00894-007-0184-9

ORIGINAL PAPER

Molecular docking study of the binding of aminopyridines within the K^+ channel

Norma Angélica Caballero · Francisco Javier Meléndez · Alfonso Niño · Camelia Muñoz-Caro

Received: 21 October 2006 / Accepted: 5 February 2007

Abstract We present a molecular docking study aimed to identify the binding site of protonated aminopyridines for the blocking of voltage dependent K^+ channels. Several active aminopyridines are considered: 2-aminopyridine, 3-aminopyridine, 4-aminopyridine, 3,4-diaminopyridine, and 4-aminoquinoleine. We apply the AutoDock force field with a lamarckian genetic algorithm, using atomic charges for the ligands derived from the electrostatic potential obtained at the B3LYP/cc-pVDZ level. We find a zone in the α-subunit of the K^+ channel bearing common binding sites. This zone corresponds to five amino acids comprised between residuals Thr107 and Ala111, in the KcsA K^+ channel (1J95 pdb structure). The 2-aminopyridine, 3-aminopyridine, 4-aminopyridine, and 3,4-diaminopyridine bind to the carboxylic oxygens of Thr107 and Ala111. In all cases aminopyridines are perpendicular to the axis of the pore. 4-aminoquinoleine binds to the carboxylic oxygen of Ala111. Due to its large size, the molecular plane is parallel to the axis of the pore. The charge distributions and the structures of the binding complexes suggest that the interaction is driven by formation of several hydrogen bonds. We find 2-aminopyridine, 3-aminopyridine, 4-aminopyridine, and 3,4-diaminopyridine with similar binding energy. Considering the standard error of the estimate of the AutoDock force field, this energy should lie, as a rough estimation, in the interval 3–7 kcal mol^{-1}. On the other hand, 4-aminoquinoleine seems to have a smaller binding energy.

Keywords Aminopyridines · K^+ channel blocking · Molecular docking · Receptor site

N. A. Caballero · F. J. Meléndez
Departamento de Fisicoquímica, Facultad de Ciencias Químicas,
Lab. de Química Teórica, Centro de Investigación,
Benemérita Universidad Autónoma de Puebla,
Edif. 139, San Claudio y 14 Sur,
Ciudad Universitaria, Puebla,
Puebla 72570, Mexico

A. Niño · C. Muñoz-Caro (✉)
Grupo de Química Computacional y Computación de Alto Rendimiento, E. S. Informática,
Universidad de Castilla-La Mancha,
Paseo de la Universidad 4,
13071 Ciudad Real, Spain
e-mail: camelia.munoz@uclm.es

Introduction

Aminopyridines are N-heterocyclic tertiary amines that inactivate the voltage-dependent K^+ channels [1–3]. Thus, the efflux of intracellular K^+ is blocked, leading to the maintenance of the pre-synaptic action potential, and consequently, increasing the nerve signal [2]. Due to this property, aminopyridines are able to reverse anaesthesia and muscle relaxation [3]. They have been also considered for the treatment of myasthenia gravis [4], multiple sclerosis [5], spinal cord injuries [6], and botulism [7]. They have also been tested for the symptomatic treatment of Alzheimer's disease [8]. In particular, 4-aminopyridine, under the name fampridine, is now being used in large-scale human trials for compensating the loss of the myelin cover in damaged nerves [9]. A recent study shows that 4-aminopyridine is slowly absorbed and eliminated [10]. This fact will allow fampridine to be administered in a convenient manner. Recently, in an attempt to identify novel compounds that restore conduction in injured spinal cord, carbamate and urea derivatives of 4-aminopiridine have been synthesized [11]. The results show that some 4-aminopyridine derivatives, like methyl and ethyl carba-

mates, maintain the ability to restore nerve function in injured nerves.

From the chemical standpoint, aminopyridines are weak bases, with pKa values around 9.0. Thus, they exist in neutral and cationic (protonated) form at physiological pH. The experimental [12–16] and theoretical evidence [17, 18] agree in that the positive charge, consequence of protonation, and one or more amino groups, suitable for hydrogen bonding, constitute the pharmacophoric pattern of aminopyridines. In this context, a functional model of activity of the K^+ channel blocking by aminopyridines has been proposed [19]. The model shows that the experimental activity index (concentration of neutral form that produces a given result) depends on the pKa and on the Gibbs energy variation (ΔG) for interaction with the receptor. Thus, knowledge of the pKa and of the interaction with the receptor is needed to fully characterize the bioactivity of aminopyridines. From these standpoints, predicting the pKa value of novel aminopyridines could be extremely useful in the search for new active molecules. In this context, a study dealing with the theoretical prediction of pKa values of aminopyridines has been presented [20]. Results show that the G1 theory level accurately predicts pKa values for aminopyridines. Considering only compounds at least as basic as pyridine (i.e., those of interest as bioactive aminopyridines) the estimated error is 0.10 and 0.12 pKa units for absolute and relative computations, respectively [20]. On the other hand, interaction of aminopyridines with the K^+ channel is not so well understood.

The K^+ channel is a tetramer exhibiting fourfold rotational symmetry (almost a C_4 point group symmetry) about a central pore [21]. Each subunit has two-transmembrane α-helices. One of the α-helix of each subunit faces the pore while the other faces the lipid membrane [21]. The overall structure resembles an inverted teepee or cone, with the narrow end in the cytoplasmic side. This structure defines the α subunit of the channel, see Fig. 1. The cytoplasmic (T1) domain of each α subunit acts as a docking platform for a β subunit. This β subunit is a tetramer of oxidoreductase proteins, and the full ensemble is arranged also in a fourfold, C_4, structure [22]. This $T1_4\beta_4$ section resembles a base for the pore in the cytoplasmic side.

X-ray data [21] shows that the pore is conformed as a tunnel about 45 Å in length. From the intracellular side, a portion of the tunnel, 18 Å in length, ends in a cavity about 10 Å width. In this zone, a K^+ ion can move and be still hydrated. This zone is large enough to admit quaternary ammonium cations, such as tetraethyl or tetrabutylammonium [23]. From the cavity to the extracellular region, the tunnel is much more narrow and a K^+ cation needs to lose its solvating water to enter.

The mechanism by which protonated aminopyridines (APH^+) inactivate the K^+ channel, as well as the physical

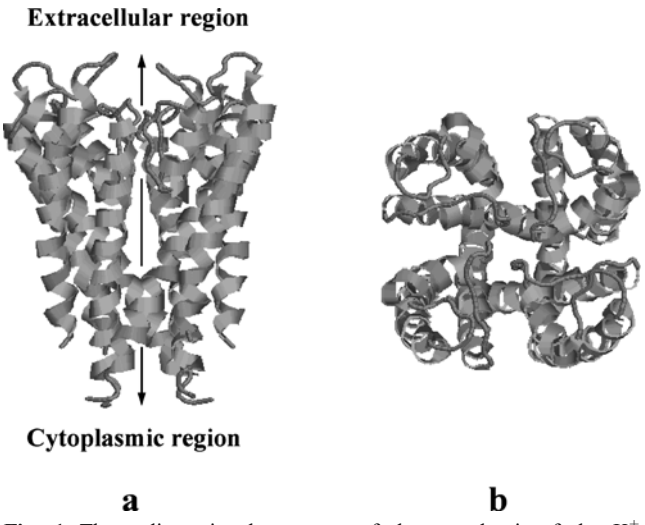

Fig. 1 Three dimensional structure of the α subunit of the K^+ channel. To the left, a front image is shown. In this draw the vertical line represents the axis of the pore. To the right, an upper view of the α subunit is shown from the extracellular side

nature of the receptor site, is not yet known. On this respect, a theoretical work [24] has proposed two putative receptor sites. The first is defined by four threonine-threonine-valine (Thr-Thr-Val) chains arranged in C_4 symmetry, with a bed of four oxygens pointing from the narrow exit channel of the pore to its large central cavity. The second proposed receptor site corresponds to four threonine (Thr) residues in the pore, with their four OH groups arranged in a square. A graphical representation of both sites can be found in reference [24].

One way to get deeper insight on this problem is to analyze the interaction between aminopyridines and the K^+ channel theoretically. Currently, there are significant research efforts in the area of protein-ligand interactions, including the development of many different techniques and the associated software tools. The primary objective is the prediction of the optimal orientation and conformation of a small molecule embedded in a protein. One of these techniques is molecular docking, which attempts to predict the structure or structures of the intermolecular complex formed between two molecules, such as a protein and a ligand [25, 26].

Solving the docking problem involves efficient search algorithms, which cover the relevant translational, rotational and conformational space. Scoring of docked protein-ligand complexes is one of the major challenges in the field of molecular docking. The purpose of the scoring procedure is the identification of protein-ligand complexes using some kind of scoring function, such as the binding energy. In addition, the procedure should give a ranking of protein-ligand complexes according to their scoring function values [27]. Initially, docking programs represented both, the receptor and the ligand, with explicit atoms. These representations make many

complex configurations possible, which all have to be evaluated. The development of molecular surface calculations and their subsequent use in docking applications significantly reduces the number of possible complexes and thus increases the speed of docking algorithms [28]. In this context, search algorithms play a key role.

There are several search algorithms trying to determine the set of possible solutions to a given problem, i.e., the search space [28]. A classical one is Simulating Annealing (SA) [29, 30]. This is a generic probabilistic meta-algorithm for the global optimization problem, which tries to obtain a good approximation to the global optimum of the given function in a large search space. On the other hand, genetic algorithms are a particular class of evolutionary algorithms that use techniques inspired by evolutionary biology such as inheritance, mutation, selection, and crossover (also called recombination) [31]. Genetic algorithms are typically implemented as a computer simulation. Here, a population of abstract representations (called chromosomes) of candidate solutions (called individuals) to an optimization problem evolves towards the best solution [28]. All these algorithms, acting on the scoring function, have been applied to the molecular docking problem, and they are implemented in different software packages.

In this work, we present a study aimed to identify the receptor site and the interactions responsible for the binding of aminopyridines in the pore of the K^+ channel. Thus, we perform a molecular docking study considering a set of bioactive aminopyridines, which have shown great ability to block the K^+ channel. The K^+ channel and the three-dimensional location and orientation of the aminopyridines is explored using a lamarckian evolutionary approach.

Methodology

The set of bioactive aminopyridines involved in this work is composed by the protonated 2-aminopyridine (2-APH^+), 3-aminopyridine (3-APH^+), 4-aminopyridine (4-APH^+), 3,4-diaminopyridine (3,4-$DiAPH^+$) and 4-aminoquinoleine (4-AQH^+). The structure of these compounds is shown in Fig. 2. For the K^+ channel we consider the X-ray structure of the KcsA K^+ channel determined at a resolution of 2.80 Å by Zhou et al. [23]. This structure is deposited in the Protein Data Bank with code 1J95. We use this structure because it is readily available, representing the most up to date determination of a K^+ channel. In this context, it is interesting to consider the observed structural conservation of K^+ channels in studies involving prokaryotic and eukaryotic systems [32, 33].

In order to carry out the docking simulations, we use the AutoDock suite as molecular-docking tool [34]. AutoDock uses a binding free-energy scoring function obtained from a fitting to a calibration set formed by 30 known protein-ligand binding constants [34]. The binding energy function includes terms for dispersion/repulsion, hydrogen bonding, electrostatics, deviation from the covalent geometry, internal rotation and global rotation and translation, desolvation and hydrophobic effects. The binding energy model implemented in AutoDock exhibits a residual standard error of 2.177 kcal mol^{-1} for the calibration set [34]. This is enough to discriminate between compounds with milli-, micro- and nano-molar inhibition constants.

AutoDock includes three search methods: simulated annealing (SA), a generic genetic algorithm (GA), and a lamarckian genetic algorithm (LGA). The GA implemented in AutoDock works by defining a population of random ligand conformations in random orientations and at random translations. The number of individuals in the population is established beforehand. The method counts the number of energy evaluations and the number of generations as the docking run proceeds, and the run terminates if either limit is reached. GA needs to set the number of the best individuals in the current population that automatically survive into the next generation, typically this is 1. The user can specify the rate of gene mutation and the rate of gene crossover. Default values are 0.02 and 0.80, respectively.

LGA is a combination of the GA method for global searching, with a local search method to perform energy minimizations. It is built on the work of Belew and Hart [35]. It has been shown that LGA represents a big improvement over the simple GA [29]. In turn, both genetic methods are much more efficient and robust than SA. All these methods use the binding energy as scoring function, trying to minimize it considering the flexibility, overall rotation and translation of the ligand [34].

The K^+ channel pdb file (1J95) has tetrabutilammonium (TBA) as ligand and four potassium ions, which are removed to have a free receptor. Using AutoDock, we added Kollman charges [36, 37] and solvation parameters to characterize the macromolecule.

The ligand must have atomic charges assigned to carry out the interaction with the K^+ channel. To such an end, we use electrostatic potential (ESP) derived charges. The electrostatic potential depends directly on the wave function. Therefore, the ESP converges as the quality of the basis set increases and higher amounts of electron correlation are recovered [38]. The electrostatic potential is sampled by placing a suitable grid of points around each nucleus with distances from just outside the van der Waals radius to about twice that distance. The atomic charges are determined as those which reproduce the electrostatic potential as closely as possible at these points, subject to the constraint that the sum of charges equals the total molecular charge [39, 40]. In the present case, we use for the protonated aminopyridines molecular structures fully

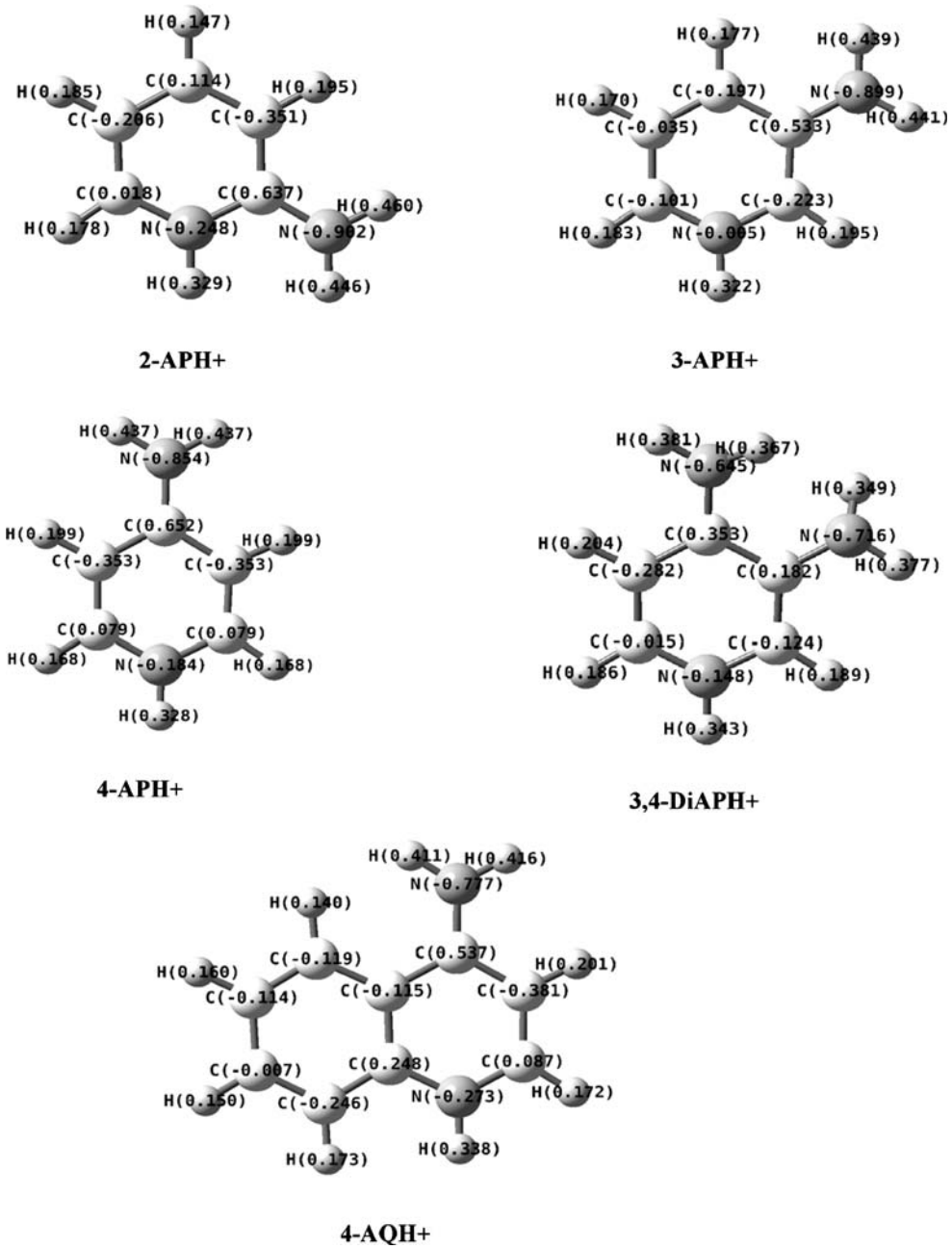

Fig. 2 Molecular structures of the protonated, bioactive, aminopyridines considered in this work. The figure includes the ESP atomic charges in atomic units (electron charge, e). All data obtained at the B3LYP/cc-pVDZ theory level

optimized at the B3LYP/cc-pVDZ theory level [18]. The ESP charges are calculated using these geometries and the same level of theory. The electronic structure calculations have been performed with the Gaussian03 package [41].

The set of protonated aminopyridines considered in this work does not have any rotatable bonds, so they do not have active torsions. Therefore, only translational and rotational degrees of freedom are considered in the docking procedure.

Interaction of the macromolecule with the ligand is performed in AutoDock by defining in the macromolecule a grid of regularly spaced points. This grid must surround the region of interest in the macromolecule. For each kind of atom in the ligand, one grid point stores the potential energy arising from interaction with all the macromolecule [42]. In the present case, the section of the K^+ pore from the central cavity to the extracellular side is too narrow for allowing aminopyridines to enter. In fact, from the X-ray data the upper entrance to the pore is found about 4 Å wide, whereas aminopyridines are about 6 Å [24]. Thus, we analyze the K^+ pore from the cytoplasmic side until the central cavity. Therefore, the grid is centred, in the macromolecule, in the point with coordinates values (referred to the 1J95 pdb structure) of 77.670 Å,

27.167 Å and 36.514 Å for the **x**, **y** and **z** axis, respectively. This represents the default grid centre taken as the geometric centre of the macromolecule obtained by averaging all its coordinates. The grid parameters used are 36, 40 and 100 points in the **x**, **y** and **z** dimension, respectively, and a grid point spacing of 0.375 Å, which is the default value.

The genetic algorithm begins by creating a random population of individuals where the number of individuals must be specified. For each individual in the initial population, a uniformly distributed random value between the minimum and maximum x, y, and z values of the grid is given for the three translations. The four genes defining the rotational orientation are given by a random quaternion, consisting of a random unit vector and a random rotation angle between −180° and +180°. The creation of the random initial population is followed by a loop over generations, repeating until a maximum number of generations (runs) or until a maximum number of energy evaluations is reached, whichever comes first [34]. In addition, the LGA approach performs a local search at each generation. In this case we consider a maximum of 100 generations. We use a starting population size of 200 individuals (a density of 0.026 individuals by $Å^3$) to increase the initial number of random orientations, to perform a deeper exploration of the translational and rotational space. We use the AutoDock default values for the remaining parameters.

Results and discussion

The zone between the entrance of the pore, in the cytoplasmic side, and the large central cavity of the K^+ channel is considered for identification of putative receptor sites for aminopyridines. The K^+ pore considered region is fully explored using the LGA evolutionary approach and the whole set of considered aminopyridines, see Fig. 2.

To characterize the ligands in the docking procedure, we compute the electrostatic potential derived charges obtained at the B3LYP/cc-pVDZ optimized geometries. Figure 2 collects the results for the considered set of aminopyridines. We observe that in all the compounds the amine nitrogens are the most electronegative atoms. The localized charge ranges between −0.902 e for 2-APH^+ and −0.645 e for the 4 amine group of 3,4-$DiAPH^+$. The most electropositive atoms are in all cases the amine hydrogens, with a localized charge value about +0.4 e. The hydrogen on the pyridinic nitrogen follows in electropositivity, with a value of localized charge about 0.3 e. These data show that the amine nitrogens, and to a lesser extend the pyridinic nitrogens with their associated hydrogens, are especially well suited to act as donors in hydrogen bonding.

After applying the molecular docking procedure to the set of considered aminopyridines, see Fig. 2, several binding sites appear. Some of these sites are located out the pore, in the cytoplasmic part of the K^+ channel. Another set corresponds to side positions within the large central cavity. However, two common binding sites within the pore of the K^+ channel are found for 2-APH^+, 3-APH^+, 4-APH^+ and 3,4-$DiAPH^+$. These binding zones are placed between the input of the intracellular side and the large central cavity of the K^+ channel, see Fig. 3. The first binding zone (FBZ) is formed by four threonine residuals (residual number 107) arranged in an approximate C_4 symmetry distribution. The second binding zone (SBZ) corresponds to four alanine residuals (residual number 111), again in an approximate C_4 symmetry arrangement. The section between the FBZ and the SBZ is defined by five aminoacids as shown in Fig. 4. It is interesting to note that the FBZ, conformed by the four Thr107 residuals, were previously identified as a putative receptor site on the basis of electronic and structural data [24]. When an aminopyridine binds to one of these docking sites, or zones, it is placed perpendicular to the pore direction. Thus, the K^+ channel is blocked. Figure 5 shows, using 2-APH^+ as illustration, the protein-ligand complex formed in the two common docking zones. In both cases, the 2-APH^+ molecular plane (as well as those of 3-APH^+, 4-APH^+ and 3,4-$DiAPH^+$) is close to the CO groups of the peptide bond. From the X-ray data, we observe that in the FBZ the four Thr107 CO oxygens define a square with an average side of 6.48 Å. On the other hand, in the SBZ the four Ala111 CO oxygens define a square with an average side of 6.78 Å.

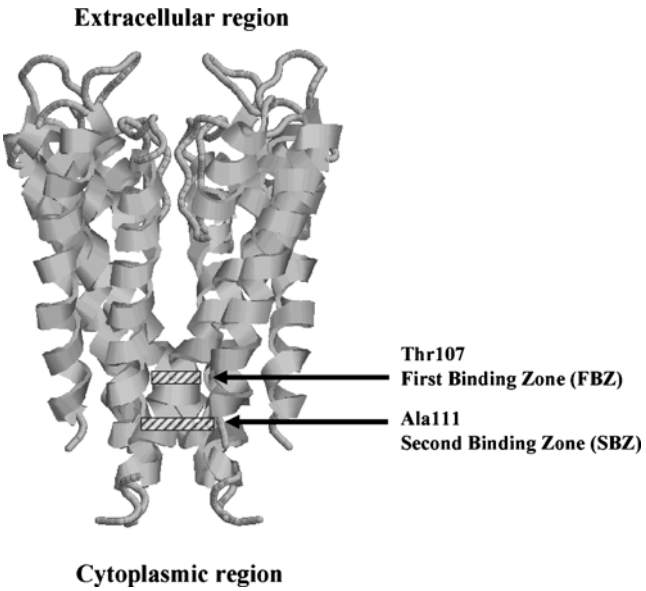

Fig. 3 Schematic representation of the two common binding sites for protonated aminopyridines in the K^+ pore, as identified by the LGA algorithm in the docking procedure. The draw depicts the tetrameric KcsA K^+ channel α-subunit

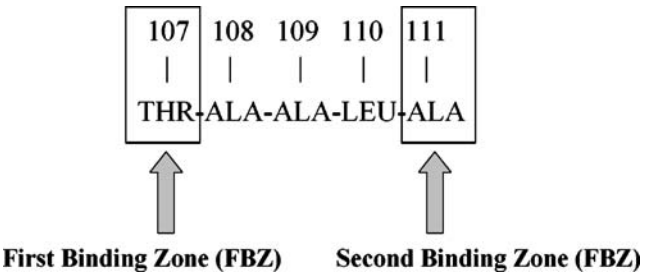

Fig. 4 Amino acid sequence of the section of the K^+ pore containing the two putative receptor sites identified in this work. Only one of the subunits conforming the tetrameric KcsA K^+ channel α-subunit is shown

On the other hand, 4-AQH^+ exhibits a slightly different behaviour. After the docking procedure, it binds within the same section defined by the FBZ and the SBZ. However, it is placed parallel to the pore direction, rather than perpendicular as the other molecules, see Fig. 6. This behaviour can be attributed to steric hindrance, with 4-AQH^+ needing to rotate in order to accommodate its larger size. Now, the N-H moieties are close to the CO groups of the SBZ. It is necessary to remark that, especially for 4-AQH^+, the flexibility of the channel could play a role in the blocking process. However, the empirical evidence shows that when the pore is blocked by tetrabutylammonium the structural change of the pore is negligible [23]. This fact suggests that a fixed pore structure, as in the present study, can be a suitable first approximation.

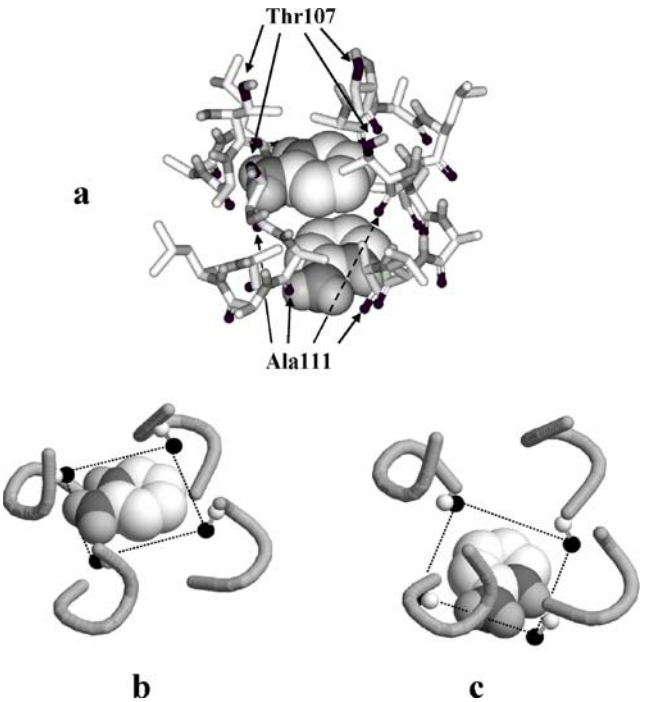

Fig. 5 Three-dimensional structure of the complex between 2-APH^+ and the binding sites of the K^+ pore. Only the amino acid sequence from Thr107 to Ala111 is considered. Case a) corresponds to the results of the docking procedure. Case b) depicts the complex of 2-APH^+ with the FBZ. Case c) depicts the complex of 2-APH^+ with the SBZ. In both cases, two different representations are included, where the black balls represent the oxygen atoms of the CO in the peptide bond. In cases b) and c) the right representation shows these oxygens as spacefilled structures. Only the most electropositive hydrogen atoms of 2-APH^+ are shown

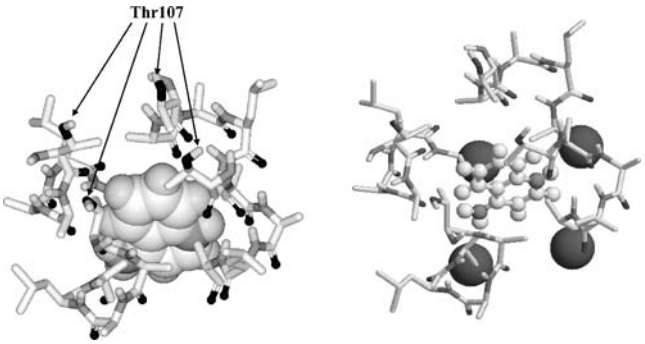

Fig. 6 Three-dimensional structure of the complex between 4-AQH^+ and the binding sites of the K^+ pore. Only the amino acid sequence from Thr107 to Ala111 is considered. Two different representations are included. In the left, the Thr107 position is marked. The right representation shows the CO oxygens of the peptide bond as spacefilled structures

Previous studies suggest that, π−cation, hydrogen bonding, and π-π interactions can be responsible for the binding of aminopyridines to the receptor site in the K^+ channel [18, 24]. However, the spatial disposition of the bound aminopyridines found in the present study suggests that several N-H···O hydrogen bonds are formed, with the CO oxygens of Thr107 or Ala111 acting as hydrogen acceptors. Thus, our findings are compatible with an interaction ligand-receptor driven essentially by hydrogen bonding. The lack of electronic information in the force field does not make possible a more detailed analysis and characterization of the interaction forces.

Table 1 collects the binding energies of the considered set of aminopyridines to the two identified binding sites. For 2-APH^+, 3-APH^+, 4-APH^+ and 3, 4-$DiAPH^+$, the binding energy is close to 5 kcal mol^{-1}, with the energy difference being small. In all cases the difference is below

Table 1 Binding energies (in kcal mol^{-1}) of the protonated aminopyridines for the two possible binding sites (FBS and SBS as defined in the text) in the K^+ channel

	Thr107 (FBZ)	Ala111 (SBZ)
2-APH^+	−4.84	−4.73
3-APH^+	−4.67	−4.58
4-APH^+	−4.66	−4.54
3, 4-$DiAPH^+$	−4.96	−4.75
4-AQH^+	–	+0.15

The data correspond to the minimum energy conformations located by a Lamarckian genetic algorithm on the AutoDock force field at a temperature of 298.15 K.

the standard error of the estimate of 2.177 kcal mol^{-1}, for the AutoDock binding energy model. Therefore, the results do not permit to discriminate between these molecules. However, taking into account the value for the error of the estimate (2.177 kcal mol^{-1}), the binding energies should lie in the interval 3–7 kcal mol^{-1}. This can only be considered as a rough estimation, since binding energies for aminopyridines are not included in the AutoDock calibration set. On the other hand, if we give a qualitative value to the present results, Table 1 shows that binding to the Thr107 site is slightly favoured over the Ala111 one. In fact, a larger number of structures are found in Thr107 than in Ala111 in the LGA searching process. Respect to 4-AQH^+ the results in Table 1 suggest that the binding energy is smaller than for 2-APH^+, 3-APH^+, 4-APH^+ and 3, 4-$DiAPH^+$.

Conclusions

In this work, a molecular docking study is performed to investigate the way by which aminopyridines block the K^+ channel. We consider a set of active (protonated) aminopyridines formed by 2-aminopyridine (2-APH^+), 3-aminopyridine (3-APH^+), 4-aminopyridine (4-APH^+), 3,4-diaminopyridine (3,4-$DiAPH^+$) and 4-aminoquinoleine (4-AQH^+).

Calculation of electrostatic potential derived atomic charges, at the B3LYP/cc-pVDZ level, shows that the amine nitrogen, on one hand, and the pyridinic nitrogens and hydrogens, on the other, are clearly electronegative and electroposite, respectively. Therefore, the N-H groups are well suited to act as hydrogen donors in hydrogen bonded complexes.

Applying an evolutionary approach to molecular docking, we identify in the α-subunit of the K^+ channel, within the pore, a common region where all the considered aminopyridines bind. Considering one of the identical tetrameric units conforming the α-subunit of the K^+ channel, this region is composed of the five amino acids between residuals number 107 and 111 (Thr107-Ala108-Ala109-Leu110-Ala111). For 2-APH^+, 3-APH^+, 4-APH^+ and 3,4-$DiAPH^+$ two binding sites are identified. The first is conformed by four oxygens, in the tetrameric structure, corresponding to the carbonyl groups of the Thr107 residuals. The second is formed by another four oxygens, in the tetrameric structure, now corresponding to the carbonyl groups of the Ala111 residuals. Aminopyridines bind to these sites in a position where the molecular plane is perpendicular to the axis of the pore. In this way, the K^+ channel is blocked. On the other hand, 4-AQH^+ is found in the same zone, but now placed with the molecular plane parallel to the axis of the pore. This is due to the larger size of this compound. Now the amine and pyridinic N-H groups are found close to the carbonyl oxygens of the Ala111 residuals.

The present results suggest that aminopyridines block the K^+ channel by forming several hydrogen bonds with the tetrameric structure formed by the four Thr107 or Ala111 residuals of the K^+ channel α-subunit.

Respect to the binding energy, we find that 2-APH^+, 3-APH^+, 4-APH^+ and 3, 4-$DiAPH^+$ have a similar value. Taken into account the standard error of the estimate in the AutoDock force field, the binding energy should lie, roughly, in the interval 3–7 kcal mol^{-1}. The results suggest that these molecules bind preferentially to the Thr107 site. On the other hand, 4-AQH^+ seems to have a smaller binding energy than the previous set of aminopyridines.

Acknowledgements The authors wish to thank the *Consejería de Educación y Ciencia de la Junta de Comunidades de Castilla-La Mancha* (grant # PBI05-009), the *Universidad de Castilla-La Mancha,* the *Ministerio de Educación y Ciencia* (grant # FIS2005-00293), the VIEP(BUAP)-CONACYT (grant # 31/g/NAT/05) and CONACYT (research fellowship 164001) for financial support.

References

1. Kirsch GE, Narahashi T (1978) Biophys J 22:507–512
2. Molgó J, Lemeignan M, Peradejordi F, Lechat P (1985) J Pharmacol (Paris) 16(Suppl. II):109–144
3. Carlssom C, Rosen I, Nilsson E (1993) Acta Anaesth Scand 27:87–90
4. McEvoy KM, Windebank AJ, Daube NJR, Low PA (1989) N Engl J Med 321:1567–1571
5. Schwid SR, Petrie MD, McDermott MP, Tierney DD, Manson DH, Goodman AD (1997) Neurology 48:817–821
6. Segal JL, Brunnemann BS (1997) Pharmacotherapy 17:415–423
7. Sellin LC (1981) Med Biol 59:11–20
8. Davidson M, Zemishlany HJ, Mohs RC, Horvath TB, Powchik P, Blass JP, Davis KL (1988) Biol Psychiat 23:485–490
9. Wickelgren I (2002) Science 297:178–181
10. Hayes KC, Potter PJ, Hsieh JT, Katz MA, Blight AR, Cohen R (2004) Arch Phys Med Rehab 85:29–34
11. Smith DT, Shi R, Borgens RB, McBride JM, Jackson K, Byrn SR (2005) Eur J Med Chem 40:908–917
12. Gillespie JI, Hutter OF (1975) J Physiol (Lond) 252:70P–71P
13. Molgó J, Lundh H, Thesleff S (1980) Eur J Pharmacol 61:25–34
14. Kirsch GE, Narahashi T (1983) J Pharmacol Exp Ther 226:174–179
15. Howe JR, Ritchie JM (1991) J Physiol 433:183–205
16. Choquet D, Korn H (1992) J Gen Physiol 99:217–240
17. Peradejordi F, Molgó J, Lemeignan M (1985) Eur J Med Chem 20:155–161
18. Niño A, Muñoz-Caro C (2001) Biophys Chem 91:49–60
19. Niño A, Muñoz-Caro C, Carbó-Dorca R, Girones X (2003) Biophys Chem 104:417–427
20. Caballero NA, Melendez FJ, Muñoz-Caro C, Niño A (2006) Biophys Chem 124:155–160
21. Doyle DA, Cabral JM, Pfuetzner RA, Kuo A, Gulbis JM, Cohen SL, Chait BT, MacKinnon R (1998) Science 280:69–77
22. Gulbis JM, Zhou M, Mann S, McKinnon R (2000) Science 289:123–127

23. Zhou M, Morais-Cabral JH, Mann S, McKinnon R (2001) Nature 411:657–661
24. Muñoz-Caro C, Niño A (2002) Biophys Chem 96:1–14
25. Brooijmans N, Kuntz ID (2003) Biomol Struct 23:335–373
26. Halperin I, Ma B, Wolfson H, Nussinov R (2002) Proteins 47:409–443
27. Krovat EM, Steindl T, Langer T (2005) Curr Comput-Aided Drug Des 1:93–102
28. Bursulaya BD, Totrov M, Abagyan R, Brooks III CL (2003) J Comput-Aided Mol Des 17:755–763
29. Goodsell DS, Olson AJ (1990) Proteins 8:195–202
30. Morris GM, Goodsell DS, Huey R, Olson AJ (1996) J Comput-Aided Mol Des 10:293–304
31. Holland JH (1975) Adaptation in natural and artificial systems. University of Michigan Press, Ann Arbor, MI
32. MacKinnon R, Cohen SL, Kuo A, Lee A, Chait BT (1998) Science 280:106–109
33. Doyle DA, Cabral JM, Pfuetzner RA, Kuo A, Gulbis JM, Cohen SL, Chait BT, MacKinnon R (1998) Science 280: 69–77
34. Morris GM, Goodsell DS, Halliday RS, Huey R, Hart WE, Belew RK, Olson AJ (1998) J Comput Chem 19:1639–1662
35. Hart WE (1994) Adaptive global optimization with local search. Ph.D. Thesis Computer Science and Engineering Department, University of California San Diego. See also: "ftp://ftp.cs.sandia.gov/pub/papers/wehart/thesis.ps.gz"
36. Singh VC, Kollman PA (1984) J Comput Chem 5:129–145
37. Besler BH, Merz KM, Kollman PA (1990) J Comput Chem 11:431–439
38. Jensen F (1999) Introduction to computational chemistry. Wiley
39. Laio A, Gervasio FL, VandeVondele J, Sulpizi M, Rothlisberger U (2004) J Phys Chem B 108:7963–7968
40. Gross KC, Seybold PG, Hadad CM (2002) Int J Quantum Chem 90:445–458
41. Gaussian 03 (2004) Frisch MJ, Trucks GW, Schlegel HB, Scuseria GE, Robb MA, Cheeseman JR, Montgomery Jr JA, Vreven T, Kudin KN, Burant JC, Millam JM, Iyengar SS, Tomasi J, Barone V, Mennucci B, Cossi M, Scalmani G, Rega N, Petersson GA, Nakatsuji H, Hada M, Ehara M, Toyota K, Fukuda R, Hasegawa J, Ishida M, Nakajima T, Honda Y, Kitao O, Nakai H, Klene M, Li X, Knox JE, Hratchian HP, Cross JB, Bakken V, Adamo C, Jaramillo J, Gomperts R, Stratmann RE, Yazyev O, Austin AJ, Cammi R, Pomelli C, Ochterski JW, Ayala PY, Morokuma K, Voth GA, Salvador P, Dannenberg JJ, Zakrzewski VG, Dapprich S, Daniels AD, Strain MC, Farkas O, Malick DK, Rabuck AD, Raghavachari K, Foresman JB, Ortiz JV, Cui Q, Baboul AG, Clifford S, Cioslowski J, Stefanov BB, Liu G, Liashenko A, Piskorz P, Komaromi I, Martin RL, Fox DJ, Keith T, Al-Laham MA, Peng CY, Nanayakkara A, Challacombe M, Gill PMW, Johnson B, Chen W, Wong MW, Gonzalez C, Pople JA, Gaussian, Inc., Wallingford CT
42. Morris GM, Goodsell DS, Huey R, Hart WE, Halliday S, Belew R, Olson AJ (2001) AutoDock version 3.0.5. User's guide. Available from: http://www.scripps.edu/mb/olson/doc/autodock/ad305/Using_AutoDock_305.html